PHYSICAL REVIEW A VOLUME 36, NUMBER 12 DECEMBER 15, 1987

# Calculation of neutron cross sections and thermalization parameters for molecular gases using a synthetic scattering function. II. Applications to $H_2O$, $D_2O$, and $C_6H_6$

J. R. Granada, V. H. Gillette, and R. E. Mayer
*Centro Atomico Bariloche and Instituto Balseiro, Comision Nacional de Energia Atomica,*
*8400 San Carlos de Bariloche, Argentina*

(Received 7 November 1986)

The formulas derived from the synthetic model which were presented in the preceding paper are here applied to the evaluation of partial and total cross sections at thermal neutron energies for the commonly used moderators $H_2O$, $D_2O$, and $C_6H_6$. The results of our analytical expressions for the scattering kernels $\sigma_0(E_0,E)$ and $\sigma_1(E_0,E)$ are compared with standard code calculations for well-separated incident neutron energies $E_0$. The related integral quantities, total cross section $\sigma(E_0)$, and average cosine of the scattering angle $\langle\cos\theta(E_0)\rangle$, respectively, are also compared with experimental data and results from other theories. Within the framework of neutron diffusion theory, transport coefficients are readily evaluated using the model expressions and they are compared with available information over a wide range of temperatures.

## I. INTRODUCTION

The synthetic scattering function $T(Q,\omega;E_0)$ introduced in a recent article[1] has been developed to describe—in an approximate way—the interaction of thermal neutrons with molecular gases. It has been devised to produce a practical answer to those problems in which a detailed knowledge of the system's frequency spectrum is unnecessary. Under these conditions a synthetic model intended to give a good representation of some integral properties of the actual (self-) scattering law, only requires retaining the main dynamical characteristics of the molecular unit.

In the preceding paper[2] we have exploited the formal simplicity of the synthetic model to derive analytical expressions for $\sigma_0(E_0,E)$ and $\sigma_1(E_0,E)$, the zero- and first-order angular moments of the double-differential cross section, respectively, as well as for the total cross section $\sigma(E_0)$. With this information at hand, several useful quantities describing neutron thermalization in a moderating media can be readily evaluated. In particular, the Boltzmann transport equation can be written completely in terms of the proposed scattering kernels, including the source term. This is so because the synthetic function itself reduces to the proper ("hot" free gas) form at epithermal incident neutron energies, thus avoiding any mismatch between cross sections evaluated at "high" or "low" energies in a multigroup calculation.

We present here the results of our formulas for the evaluation of some quantities of interest in reactor physics, exemplified through the commonly used moderators $H_2O$, $D_2O$, and $C_6H_6$. Light water and benzene are a natural choice to test the essentially incoherent synthetic model as the proton scattering plays a dominant role. On the other hand, although coherence effects are important in neutron scattering by heavy water, the incoherent approximation is still useful to describe many thermalization and transport properties in this system.[3]

In Sec. II we compare our partial and total cross sections with experimental data and those obtained from other theories, whereas neutron diffusion parameters over a wide range of temperatures are given in Sec. III. Although the synthetic scattering function does not pretend to be a real scattering law for molecules, we compare in Sec. IV its predictions with some observed double-differential cross sections. For the sake of completeness, we also show some calculated angular distributions, although inelasticity corrections using this model for the cases of reactor and pulsed neutron sources have been discussed elsewhere.[4]

The input data for all the calculations presented here are summarized in Table I. In addition, we have used the values $\sigma_b^{H}=81.66b$, $\sigma_b^{D}=7.63b$, $\sigma_b^{C}=5.551b$, $\sigma_b^{O}=4.232b$, and $\sigma_{abs}^{H}(2200\text{m/sec})=0.3326b$ for the required bound-atom and absorption cross sections. A preliminary account of some of these results has been given elsewhere.[5]

TABLE I. Values of the parameters for the synthetic model used in the calculations. Energies are given in eV and masses in neutron mass units.

| Atom | $H_2O$ | | $D_2O$ | | $C_6H_6$ | |
|---|---|---|---|---|---|---|
| Parameter | H | O | D | O | H | C |
| $\hbar\omega_1$ | 0.070 | | 0.050 | | 0.120 | |
| $\hbar\sigma_1$ | 0.021 | | 0.021 | | 0.030 | |
| $M_1$ | 2.380 | 342.0 | 4.390 | 190.5 | 1.531 | 17.67 |
| $\hbar\omega_2$ | 0.205 | | 0.150 | | 0.380 | |
| $\hbar\sigma_2$ | 0.018 | | 0.018 | | 0.018 | |
| $M_2$ | 4.768 | 746.2 | 13.25 | 427.4 | 3.345 | 392.3 |
| $\hbar\omega_3$ | 0.481 | | 0.310 | | | |
| $\hbar\sigma_3$ | 0.018 | | 0.018 | | | |
| $M_3$ | 3.180 | 373.1 | 6.817 | 203.7 | | |

## II. NEUTRON CROSS SECTION

### A. The energy-transfer kernels

Besides the scattering function itself, the most basic quantities of interest in neutron thermalization studies are the lower-order coefficients in the expansion of $d^2\sigma/d\Omega\, dE$ in Legendre polynomials,

$$\sigma_l(E_0,E)=2\pi\int_{-1}^{1} d(\cos\theta)P_l(\cos\theta)\frac{d^2\sigma}{d\Omega\, dE}\ . \qquad (1)$$

Although analytical expressions for all these scattering kernels can be obtained from the synthetic model, we will only consider here the first two as they form the basis for the widely used $P_1$ approximation.[6]

In Fig. 1 we show the results of our formula [Eq. (23), Ref. 2] for the isotropic energy-transfer kernel, $\sigma_0(E_0,E)$, corresponding to light water at room temperature. They are compared with GASKET–FLANGE calculations[7–9] at three well-separated incident neutron energies and for a wide range of final energies. Even though some discrepancies are apparent, a good overall agreement is observed. We show in Fig. 2 the same kind of calculations, but in this case performed for $D_2O$ at room temperature; as before, there is good agreement between both evaluations. The contribution due to annihilation of rotational "phonons" is clearly seen in the upscattering side of the kernels corresponding to the lowest incident neutron energy. At higher values of $E_0$, these contributions are smeared out by the larger recoil energy associated with the smaller effective mass of the scatterers.

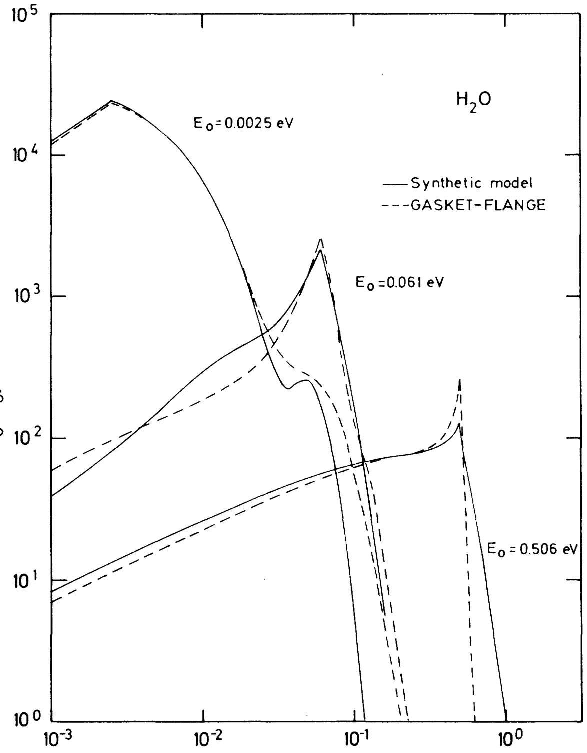

FIG. 1. The $P_0$ energy-transfer kernel of $H_2O$ at 20 °C. Results are shown for three well-separated incident neutron energies. Evaluations according to the analytical expression derived from the synthetic model (solid lines) are compared with GASKET–FLANGE calculations (dashed lines).

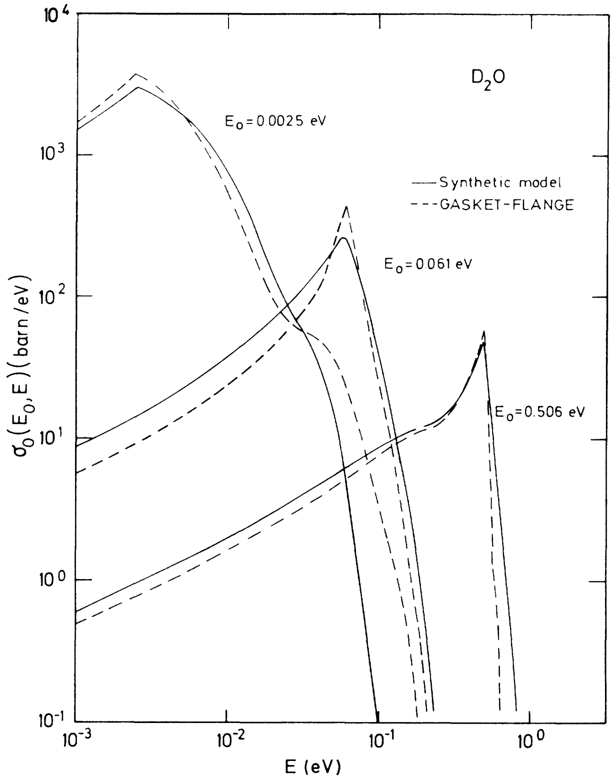

FIG. 2. The $P_0$ energy-transfer kernel of $D_2O$ at 20 °C. Other notation as in Fig. 1.

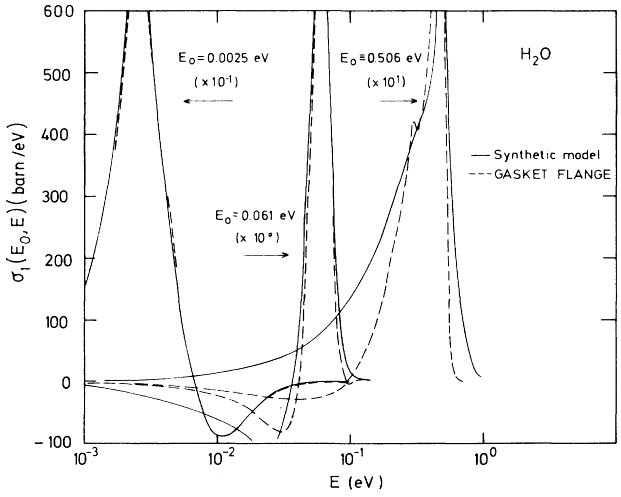

FIG. 3. The $P_1$ energy-transfer kernel of $H_2O$ at 20 °C. Other notation as in Fig. 1. Note the different scale used for each incident neutron energy.

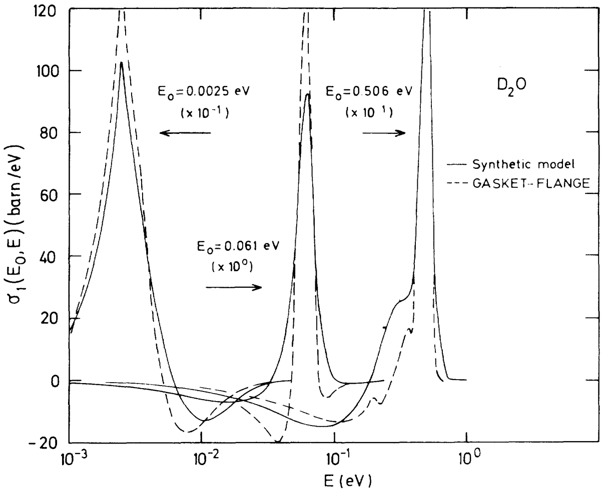

FIG. 4. The $P_1$ energy-transfer kernel of $D_2O$ at 20 °C. Other notation as in Fig. 3.

The first anisotropic energy-transfer kernel $\sigma_1(E_0,E)$ is shown in Figs. 3 and 4 for $H_2O$ and $D_2O$, respectively; as before, the result of the synthetic model expressed by Eq. (27) of Ref. 2 is compared in each case with GASKET–FLANGE calculations[9] at different incident neutron energies (note the correspondingly different scale factors in those graphs). Once again, the agreement between both calculations is encouraging, although a heavier effective mass for the lighter atom (H,D) is apparent in the GASKET–FLANGE calculation, more noticeable at the higher $E_0$.

### B. Integral cross sections

Having shown the behavior of the $P_0$ and $P_1$ scattering kernels, we will discuss now the results of the synthetic model for the related integral quantities, total cross section, and average cosine of the scattering angle, respectively. Besides the fact that they can be directly compared with experimental data, thus providing a stringent test to the bound-atom model, many useful thermalization parameters can be readily evaluated once these magnitudes are known over the thermal neutron region.

The analytical expression of the total cross section, $\sigma(E_0)$, derived from the synthetic function $T(Q,\omega;E_0)$ has been presented in Sec. IV A of Ref. 1 and Sec. III B of Ref. 2, whereas some examples of its application over the whole thermal range have been also given elsewhere.[1,5] Of course, using that expression is equivalent to numerically integrating $\sigma_0(E_0,E)$ over a (thin) final energy mesh.

In Fig. 5 we show the total cross section of $H_2O$ at room temperature over the thermal energy region. The

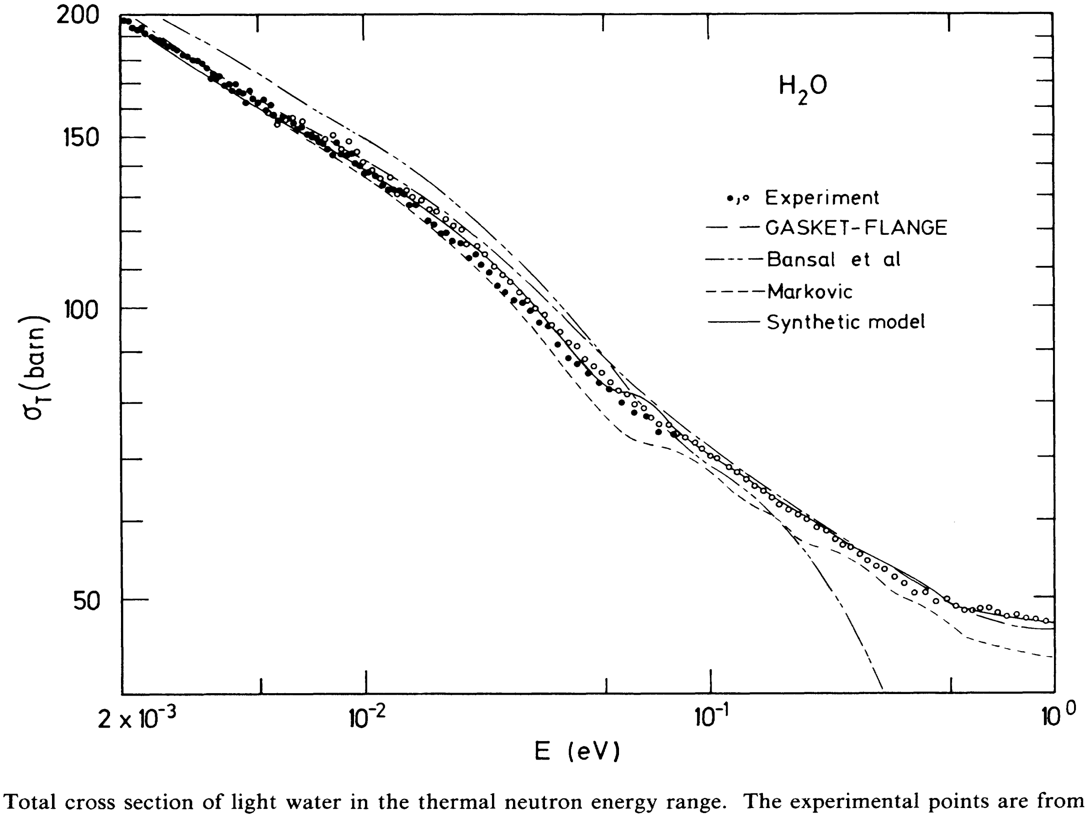

FIG. 5. Total cross section of light water in the thermal neutron energy range. The experimental points are from Refs. 10 and 11. Results of using the analytical expression derived from the synthetic model are compared with other calculations (Refs. 7, 15, and 16).

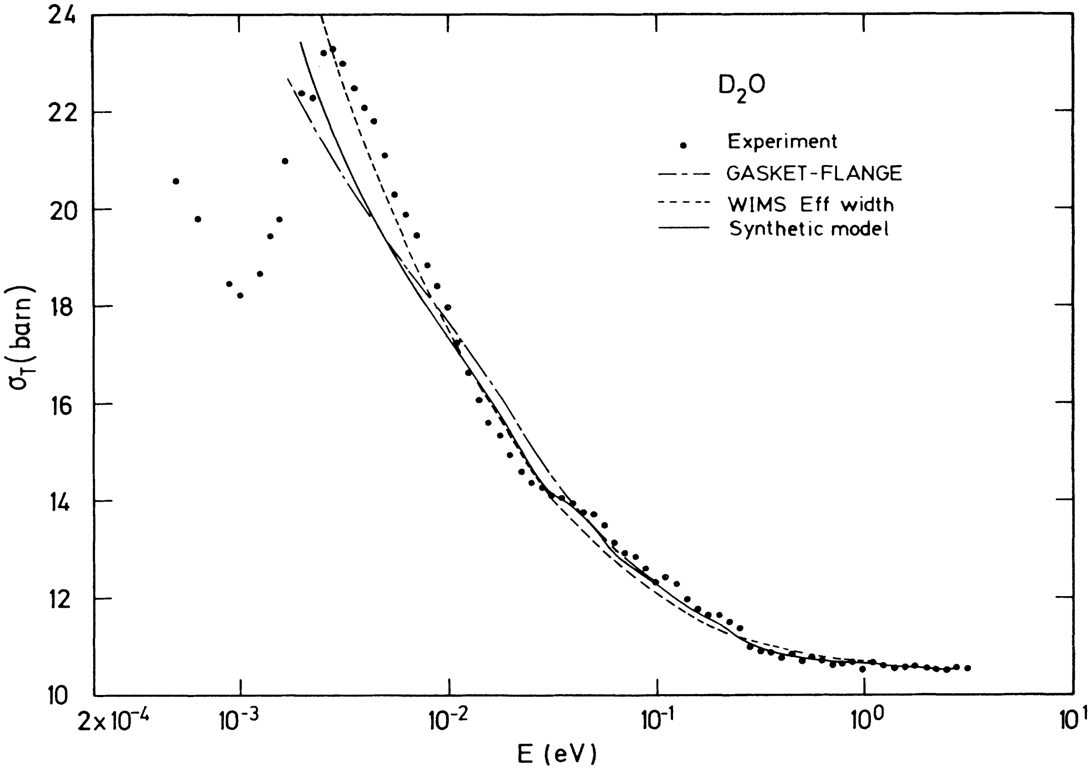

FIG. 6. Total cross section of heavy water in the thermal neutron energy range. The experimental points are from Ref. 17. The results from the model are also compared with calculations from Refs. 7 and 18.

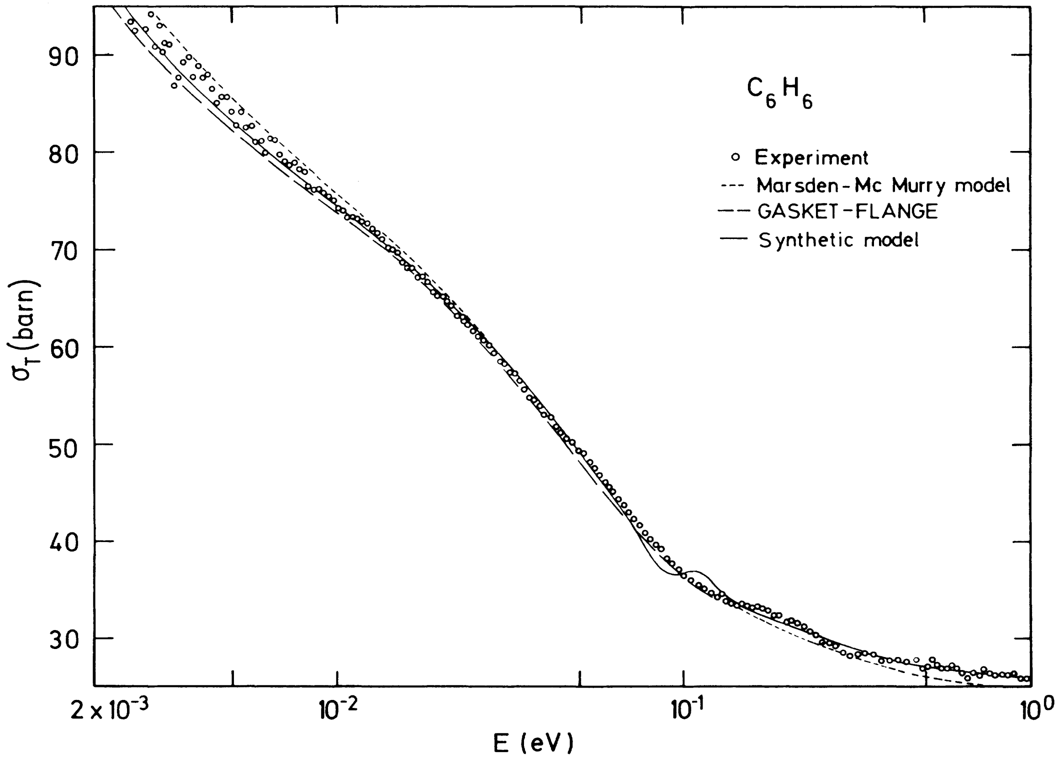

FIG. 7. Total cross section of benzene at thermal neutron energies. The experimental points are from Ref. 19. Our evaluated curve is also compared with calculations from Refs. 7 and 20.

experimental points are from Herdade *et al.*[10] and Neill, Russell, Jr., and Brown.[11] The results from the synthetic model are in excellent agreement with the data, except at very low energies ($\sim 10^{-3}$ eV, see Fig. 1, Ref. 1) where some discrepancy becomes apparent. Such a disagreement is not unexpected, however, as the experimental time scale in this range is comparable to that characteristic of the diffusive motion in the liquid. In these circumstances, the assumed free translation to represent the actual motion of the molecular unit becomes inadequate. The observed structure in the vicinity of the "rotational" eigenfrequency ($\sim$0.06 eV) is characteristic of the model and occurs around all molecular eigenfrequencies, being more noticeable in those cases where the actual frequency spectrum is a broad band. The hypothesis of an isotropic Einstein oscillator is then a crude approximation to the real situation and one can hardly expect that a single phononlike term as expressed by $\Lambda$ [Eqs. (31) and (33), Ref. 2] could properly account for what it is in fact a convolution of this type of effect. Also shown in Fig. 5 is the result of a GASKET–FLANGE calculation,[7] which is based on a continuous (Haywood II) frequency spectrum and it is contained in the thermal scattering library of the Evaluated Nuclear Data File (ENDF/B) system.[12] It must be emphasized that this latter calculation gives a $\sigma_T(E)$ which is marginally better than that from the classical Nelkin model[13] and its anisotropic version.[14] For completeness, the total cross sections corresponding to the recent water models of Bansal, Tewari, and Kothari[15] and Markovic[16] are also included in this figure.

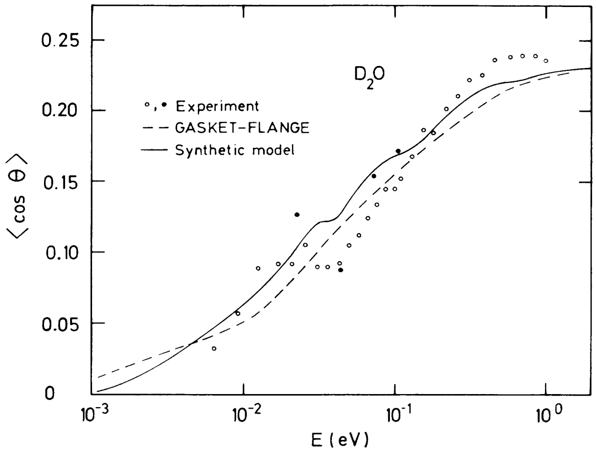

FIG. 9. The average cosine of the scattering angle for heavy water at thermal energies. The experimental points are from Refs. 23 (solid circles) and 24 (open circles). The result of our evaluation is also compared with GASKET–FLANGE calculations.

The total cross section of heavy water at room temperature is shown in Fig. 6 over the thermal energy range. The experimental points are from Kropff, Latorre, Granada, and Castro Madero.[17] The results from the synthetic model are compared with evaluations using the GASKET–FLANGE and WIMS computer codes, the latter based on its "effective width model" option in this case.[18] Large coherent contributions dominate the behavior of $\sigma_T(D_2O)$ at low energies and therefore those incoherent calculations can only give the baseline ("pedestal") over which the interference effects are superimposed. As it is shown in Sec. III, however, the synthetic model is able to produce neutron thermalization results for heavy water which are in good agreement with the most precise available measurements, as well as

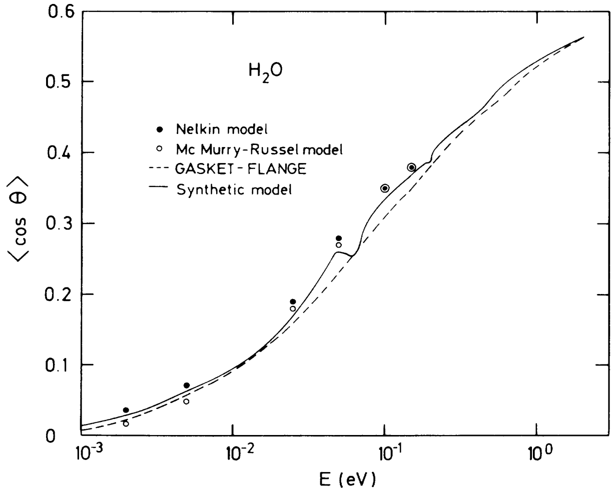

FIG. 8. The average cosine of the scattering angle for light water at thermal energies. The solid line is the results of the present model; the dashed line is a GASKET–FLANGE calculation, whereas the symbols indicate results from the Nelkin (solid circles) and McMurry (open circles) models.

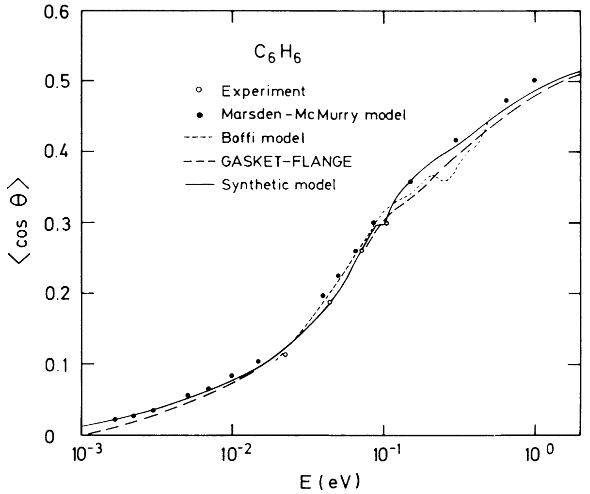

FIG. 10. The average cosine of the scattering angle for benzene at thermal energies. The experimental points (open circles) are from Ref. 25. Other calculations based on the Marsden and McMurry (Ref. 20) and Boffi (Ref. 26) models are also shown, together with the results from GASKET–FLANGE and synthetic model evaluations.

to provide an adequate description of inelasticity effects in neutron diffraction work.[4]

Figure 7 shows the total cross section of benzene for thermal neutrons. The experimental data are from Sprevak, Borgonovi, Carriveau, and Neill.[19] Our calculation is also compared with GASKET–FLANGE results[7] and an evaluation performed by Marsden and McMurry based on a different frequency spectrum.[20] Besides the feature observed in the vicinity of 0.1 eV which is caused by the reason already discussed in the case of $H_2O$ above, the synthetic scattering function gives a very good description of the $\sigma_T(C_6H_6)$ over the whole thermal energy region.

The average cosine of the scattering angle, defined by

$$\langle \cos\theta(E_0) \rangle = \frac{\int dE\, \sigma_1(E_0,E)}{\int dE\, \sigma_0(E_0,E)} = \frac{\sigma_1(E_0)}{\sigma(E_0)} , \qquad (2)$$

is another integral quantity of interest in reactor-physics calculations, as it permits the derivation of several transport magnitudes. It is shown in Fig. 8 for $H_2O$ at room temperature, as calculated according to the Nelkin,[13] McMurry-Russell,[21] and synthetic models, together with the GASKET–FLANGE results. The latter closely follow the experimental data,[22] and it is fairly well described by our evaluated curve. The situation for $D_2O$ is shown in Fig. 9, where our results are compared with the experimental points of Kornbichler[23] and Beyster[24] and the GASKET–FLANGE calculation. As in the case of the total cross section, the evaluated curves cannot properly describe the observed behavior of $\langle \cos\theta \rangle$ in heavy water due to their incoherent character. Nevertheless, its absolute value is small enough to ensure that the transport magnitudes derived from it will not be significantly affected by such discrepancy. As a final example, we show in Fig. 10 the average cosine of the scattering angle for benzene at room temperature. Once again, our evaluation is in good agreement with the GASKET–FLANGE results and the experimental data of Hofmeyr.[25] For comparison, theoretical values given by Marsden and McMurry[26] and Boffi, Marsico, Molinari, and Scozzafava[26] are also included in this figure.

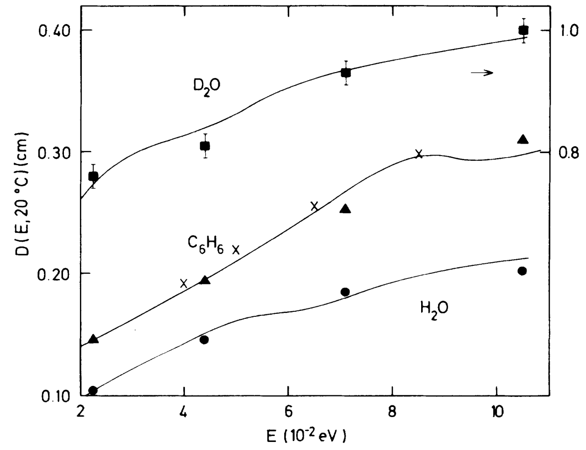

FIG. 11. The energy-dependent diffusion coefficient at 20 °C. The experimental points are from Refs. 23, 25, and 27. The solid curves are the results from the synthetic function. The crosses indicate evaluated points for benzene according to the model of Marsden and McMurry (Ref. 20).

## III. NEUTRON DIFFUSION PARAMETERS

We present in this section the results of using the formulas given in Sec. III C of Ref. 2 for the evaluation of several transport magnitudes in the molecular systems under consideration.

TABLE II. Measured and calculated values of diffusion parameters of $H_2O$ at 20 °C.

| Reference | $\bar{v}\,\overline{\Sigma}_a$ ($sec^{-1}$) | $D_0$ ($cm^2/sec$) | $C$ ($cm^4/sec$) | $T$ (°C) |
|---|---|---|---|---|
| | | Experimental values | | |
| 28 | 4883±16 | 361 50±202 | 5463±425 | 22 |
| 29 | | 360 40±180 | 3213±110 | 22 |
| 30 | 4815±53 | 359 60±555 | | 20 |
| 31 | 4886±10 | 361 80±78 | 3010±80 | 21 |
| 32 | | 357 00±400 | 3310±150 | 20 |
| 33 | 4830±65 | 364 65±390 | 4280±410 | 21.7 |
| 34 | 4817±29 | 360 10±650 | 3700±620 | 24.5 |
| 35 | 4883 | 365 91 | 2770 | Room |
| 36 | 4859±123 | 362 70±1360 | 5940±3150 | 22 |
| | | Calculated values | | |
| 37 | 4829 | 355 36 | 3224 | 22 |
| 38 | 4817 | 360 68 | 2973 | 20 |
| 39 | | 365 16 | 2920 | 22.3 |
| 40 | | 370 45 | 3361 | 20 |
| 41 | 4889 | 375 70 | 3380 | 23 |
| This work[a] | 4885 | 363 10 | 3036 | 20 |

[a] We used $\rho(20\,°C) = 0.997\,62\ g/cm^3$.

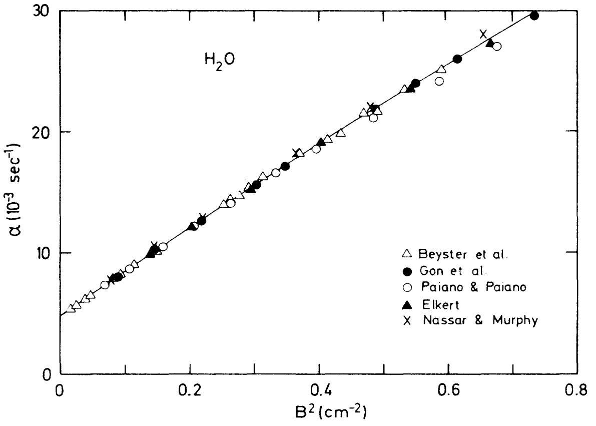

FIG. 12. The fundamental decay constant $\alpha$ as a function of the buckling $B^2$ for light water at room temperature. The measured values are from Refs. 24, 28, 33, 34, and 43. The solid line is the result of the synthetic model according to Eq. (3) with the parameters quoted in Table II.

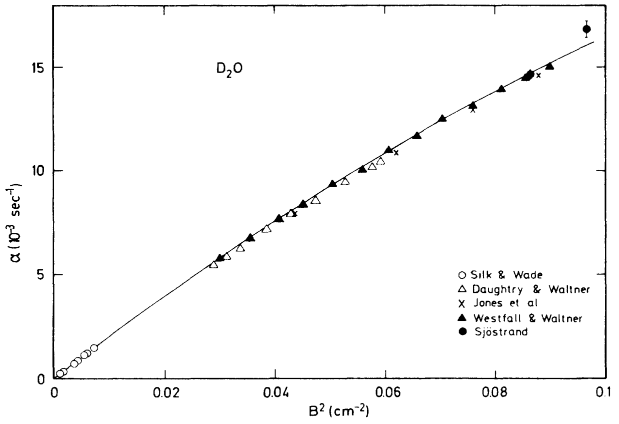

FIG. 13. The fundamental decay constant $\alpha$ for heavy water at room temperature. The measured values are from Refs. 44, 46, 47, 50, and 57. The solid line is the result of the synthetic model with the parameters quoted in Table III.

### A. Room-temperature data

There is a large amount of information on neutron diffusion parameters in hydrogeneous molecular systems, in many cases motivated by their potential use as moderators in multiplying assemblies. Most of the experiments were performed at room temperature, thus prompting the corresponding calculations at the same temperature. We show in Fig. 11 the energy-dependent diffusion coefficient $D(E,20\,°\mathrm{C})$ [Eq. (43), Ref. 2], calculated from the synthetic model over the energy range where experimental data exist[23,25,27] for the molecules we are considering here. The agreement is fairly good for light and heavy water, whereas in the case of benzene a somewhat exaggerated structure show up in our evaluation in the vicinity of 0.1 eV, due to the oscillation in the total cross section around that energy. Also shown in Fig. 11 are the calculated points of Marsden and McMurry[20] for benzene at 22 °C.

In Table II we present neutron diffusion parameters of light water at 20 °C. It contains some experimental results for the diffusion constant $D_0$ and cooling constant $C$ [Eqs. (44) and (47), Ref. 2]; a more comprehensive account of (older) experimental information can be found in Refs. 18 and 28. Data taken at a slightly different

TABLE III. Measured and calculated values of diffusion parameters of D$_2$O near room temperature.

| Reference | $\bar{v}\Sigma_a$ (sec$^{-1}$) | $10^{-5}D_0$ (cm$^2$/sec) | $10^{-5}C$ (cm$^4$/sec) | $T$ (°C) |
|---|---|---|---|---|
| | | Experimental values | | |
| 23 | | 2.09±0.015 | | 21 |
| 32 | | 2.09±0.02 | 6.6±0.3 | 20 |
| 44 | 9.56 | 2.044±0.006 | | 25 |
| 45 | 20 | 2.00±0.05 | 3.8±0.9 | 22 |
| 46 | | 1.983±0.029 | 4.65±0.54 | 25 |
| 47 | 19±2.5 | 1.97±0.14 | 3.56±1.08 | 21 |
| 48 | 10 | 2.045±0.044 | 4.706±0.381 | 21 |
| 49 | 19.0±2.0 | 2.01±0.01 | 5.15±0.25 | 22 |
| 50 | 0 | 2.039±0.013 | 4.18±0.18 | 28 |
| 51 | | 2.09±0.02 | | 20 |
| 52 | 0 | 2.08±0.05 | 3.72±0.50 | 20 |
| | | Calculated values | | |
| 53 | 19[a] | 1.98 | 5.5 | 20 |
| 54 | 9.66 | 2.02 | 3.62 | 23 |
| 55 | | 2.057 | 4.73 | 20 |
| 56 | 9.0 | 1.93 | 4.9 | 20 |
| This work[b] | 8.97 | 2.057 | 4.10 | 20 |

[a] Adopted value.

[b] We used $\rho$ (20 °C) = 1.105 g/cm$^3$.

TABLE IV. Measured and calculated values of diffusion parameters of $C_6H_6$ near room temperature.

| Reference | $\bar{v}\bar{\Sigma}_a$ (sec$^{-1}$) | $10^{-3}D_0$ (cm$^2$/sec) | $10^{-3}C$ (cm$^4$/sec) | $T$ (°C) |
|---|---|---|---|---|
| | | Experimental values | | |
| 60 | 2974±14 | 50.36±0.20 | 15.45±0.34 | 20.4 |
| 61 | 2933±25 | 49.39±0.50 | 16.93±2.20 | 20 |
| 25 | | 51.48±0.70 | | 21 |
| 36 | 2886±111 | 48.65±1.37 | 13.87±3.85 | 22 |
| 62 | 3120±50 | 48.50±0.80 | 13.30±2.40 | 20 |
| | | Calculated values | | |
| 63 | | 51.0 | 23.615 | Room |
| 64 | 2969 | 55.23 | 12.97 | 21 |
| 65 | 3010 | 52.04 | 15.70 | 21 |
| 20 | 2973 | 52.50 | 17.20 | 22 |
| This work[a] | 3013 | 51.488 | 16.17 | 20 |

[a] We used $\rho$ (20 °C) = 0.879 g/cm$^3$.

temperature have been corrected to 20 °C using the coefficient $dD_0/dT = 132$ cm$^2$/sec °C as obtained from the synthetic model. Calculated values from different theories are also included in this table. Large discrepancies are evident among experimental data and even between evaluated results, and therefore we can only say that the values obtained from the synthetic model are consistent with the most precise experimental results[28,29,31] and with those calculations[38,39,42] which are based on a modified version of the Nelkin model. Most of the data quoted in Table II have been derived from pulsed neutron experiments, measuring the decay of the fundamental mode of the neutron field

$$\alpha(B^2)=\bar{v}\bar{\Sigma}_a+D_0B^2-CB^4 \tag{3}$$

over a range of values of the buckling $B^2$. We compare in Fig. 12 our calculated curve with some measurements of the decay constant in $H_2O$ at room temperature. Other quantities derived from the model are the diffusion length $\bar{L}$ and the second moment of the energy transfer $M_2$, Eqs. (46) and (48) of Ref. 2, respectively, as well as the thermalization time defined by[58]

$$t_{\text{th}}=3(\bar{v}N_m M_2)^{-1} \ . \tag{4}$$

Our calculated values for $H_2O$ at 20 °C are $\bar{L}=2.726$ cm, $M_2=91.18b$, and $t_{\text{th}}=3.97$ $\mu$sec, in very good agreement with experimental results.[18,59]

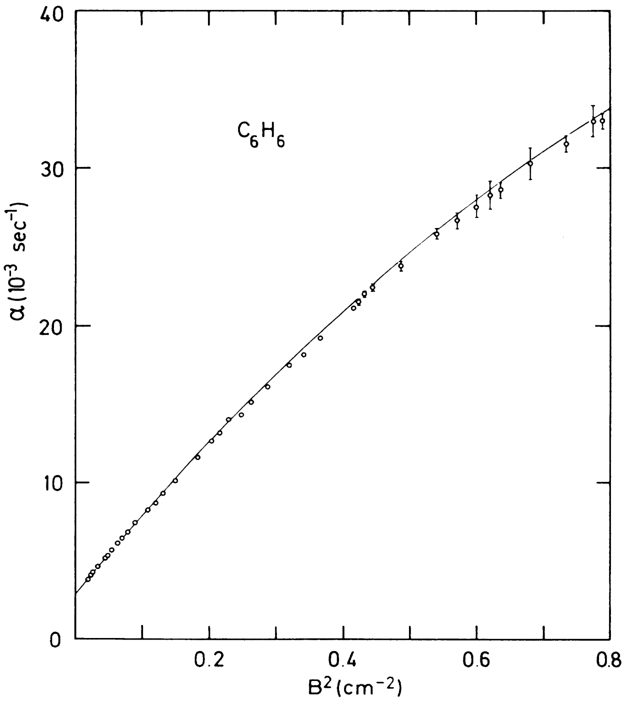

FIG. 14. The fundamental decay constant for benzene at room temperature. The experimental points are from Ref. 60. The solid line is the result of the synthetic model through the parameters quoted in Table IV.

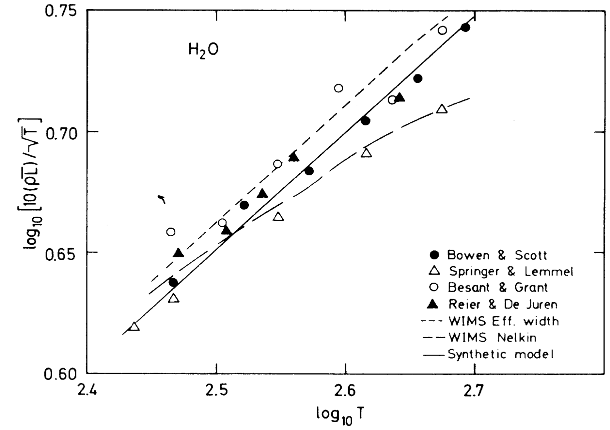

FIG. 15. Logarithmic plot of the neutron diffusion length of $H_2O$ after density removal. The measured values are from Bowen and Scott (●), Springer (△), Besant and Grant (○), and Reier and DeJuren (▲), as cited in Ref. 18. The synthetic model result (solid line) is also compared with WIMS calculations.

TABLE V. The evaluated density-removed diffusion and cooling constants of $H_2O$, $D_2O$, and $C_6H_6$ at different temperatures.

|  | $H_2O$ |  | $D_2O$ |  | $C_6H_6$ |  |
|---|---|---|---|---|---|---|
| $T$ (°C) | $10^{-4}D_0^*$ (cm$^2$/sec) | $10^{-3}C^*$ (cm$^4$/sec) | $10^{-5}D_0^*$ (cm$^2$/sec) | $10^{-5}C^*$ (cm$^4$/sec) | $10^{-4}D_0^*$ (cm$^2$/sec) | $10^{-4}C^*$ (cm$^4$/sec) |
| 20 | 3.622 | 3.015 | 2.273 | 5.529 | 4.527 | 1.099 |
| 40 | 3.864 | 3.243 | 2.381 | 5.762 | 4.838 | 1.145 |
| 60 | 4.106 | 3.479 | 2.486 | 5.989 | 5.151 | 1.193 |
| 80 | 4.348 | 3.718 | 2.589 | 6.205 | 5.465 | 1.242 |
| 100 | 4.589 | 3.958 | 2.690 | 6.412 | 5.781 | 1.293 |

Diffusion parameters for heavy water at room temperature are presented in Table III. Once again a considerable spread in the values is evident, certainly well outside the quoted errors. Our calculated value of the diffusion constant is, however, in good agreement with the weighted mean value $(2.034\pm0.032)\times10^5$ cm$^2$/sec of the experimental data at 20 °C.[18] In Fig. 13 we show our evaluated decay constant for $D_2O$ at room temperature, together with experimental points quoted over that buckling range. The results from the synthetic model for the diffusion length and the second energy transfer moment at 20 °C are $\bar{L}=151.43$ cm and $M_2=11.93b$, respectively, while the thermalization time comes out to be 30.5 $\mu$sec, in excellent agreement with the experimental results.[59]

Measured and calculated values of diffusion parameters in benzene at room temperature are summarized in Table IV. Our results are in fairly good agreement with the most recent measurement[60] and also with GASKET–FLANGE based calculations employing Sprevak's frequency spectrum.[64,65] In Fig. 14 we compare our evaluated decay constant curve with the experimental points of Lolich and Abbate.[60] Also, we have obtained the values

$$\bar{L}=4.134\text{ cm},\quad M_2=31.44b,\quad\text{and}\quad t_{\text{th}}=9.45\ \mu\text{sec}$$

for $C_6H_6$ at 20 °C.

### B. Temperature dependence

A full calculation with the synthetic model at a given temperature takes about 3 min of CPU time on a VAX 11/780, including the evaluation of cross sections, $P_0$ and $P_1$ scattering kernels (each a matrix of $80\times150$), and diffusion parameters. Temperature-variation studies can then be undertaken effortlessly, and we present in

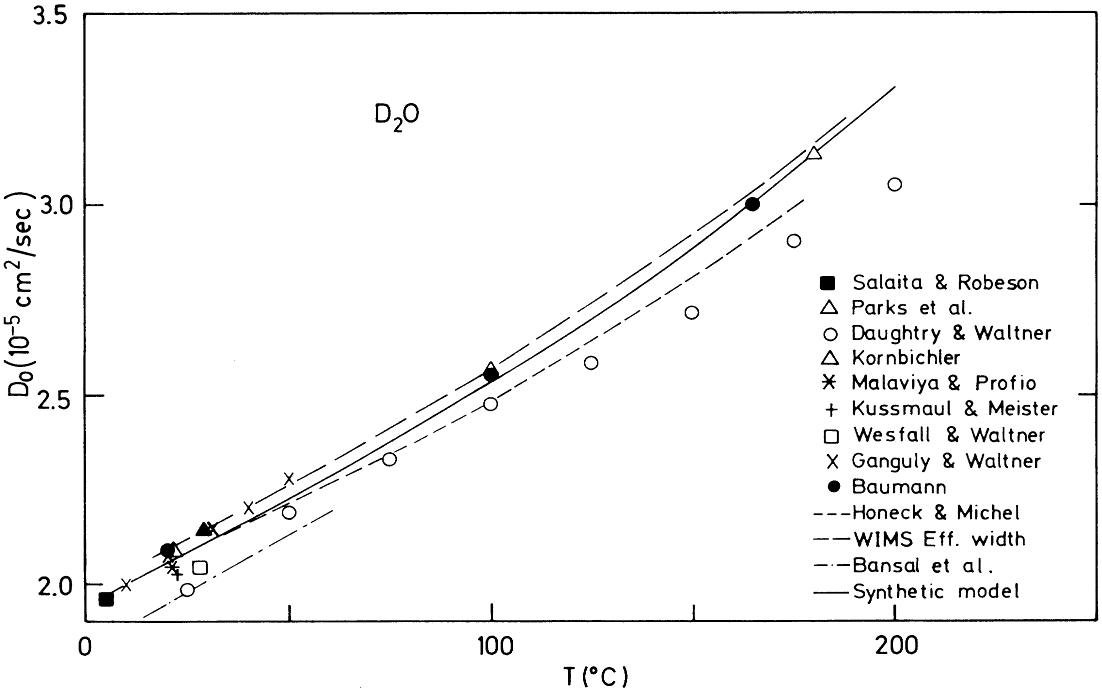

FIG. 16. The diffusion constant of $D_2O$ as a function of temperature. The experimental points are from Refs. 32 and 46–52, whereas other theoretical results are from Refs. 18, 53, and 55. The solid line is the result from the synthetic scattering function.

Table V our calculated density-removed parameters:

$$D_0^*(T)=\rho(T)D_0(T),\quad C^*(T)=\rho(T)C(T) \tag{5}$$

up to a temperature of 100 °C. In a recent publication[66] we have presented our model calculations for $H_2O$ and $D_2O$ over a much extended range of temperatures.

With the notation

$$\alpha_0^+ \equiv \bar{v}\,\bar{\Sigma}_a/\rho(T) \tag{6}$$

and the values

$$\alpha_0^+(H_2O)=4897\ (\text{cm}^3/\text{g sec})\ ,$$

$$\alpha_0^+(D_20)=8.121\ (\text{cm}^3/\text{g sec})\ ,$$

$$\alpha_0^+(C_6H_6)=3427\ (\text{cm}^3/\text{g sec})\ ,$$

obtained from the model, all the parameters entering into the decay constant expression, Eq. (3), can be generated through Eqs. (5) and (6), using the density of the normal liquids at a given temperature or any effective density which may be of interest in a special problem. Furthermore, the neutron diffusion length at any temperature can be obtained as

$$\bar{L}(T)=\rho^{-1}(T)[D_0^*(T)/\alpha_0^+]^{1/2}\ . \tag{7}$$

In Fig. 15 we show the behavior of this quantity for $H_2O$ after density removal, compared with other theories and some measured values.[18] Although there is a large spread in the data, the general trend is well described by our evaluation; in fact, the agreement with the experimental points of Bowen and Scott[30] is very good.

The diffusion constant of heavy water over a wide range of temperature is shown in Fig. 16. Our evaluated curve[67] is in very good agreement with the high-temperature data from Kornbichler[23] and Baumann,[51] whereas those from Daughtry and Waltner[46] are consistently lower than the other sets. Calculations based on a model of the Nelkin type[55] coincide with our results at room temperature, but give values which are lower than ours at higher temperatures. The results from the effective width model cannot be regarded as an independent piece of information, since the effective width parameter has been adjusted[18] to reproduce the data of Baumann.

## IV. OTHER RESULTS

In the previous sections we have presented examples of the synthetic model results for $H_2O$, $D_2O$, and $C_6H_6$, evaluated according to the formulas given in the preceding paper.[2] These applications were mainly concerned with energy-transfer kernels and their corresponding integral magnitudes, total cross sections, and thermalization parameters. They are usually the quantities of interest in reactor-physics calculations, a field in which the model seems to offer a powerful tool by providing analytical expressions for several of those central quantities.

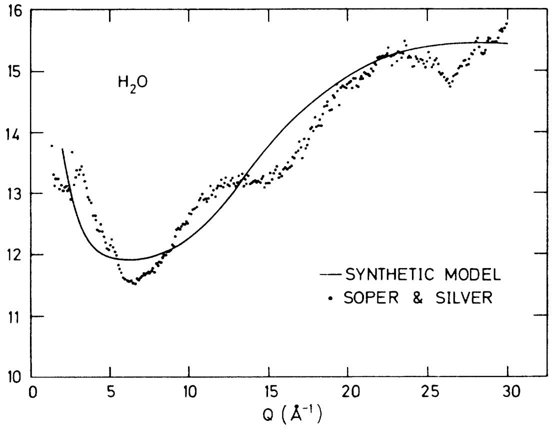

FIG. 17. Time-of-flight differential cross section of $H_2O$ as observed by Soper and Silver (Ref. 71) on a 40° detector bank. The model evaluation corresponding to the conditions of that experiment is indicated by the solid line.

There are, however, other applications of our scattering kernel which involve different problems related to slow neutron-molecule interaction. One of those is the evaluation of inelasticity corrections[68] in thermal neutron scattering experiments on molecular liquids, to account for unavoidable nonelastic processes which affect the observed structure factor. In the case of light mass scatterers, the classic Placzek[69] expansion breaks down and the treatment of these effects becomes difficult. We have recently used the synthetic model to evaluate those corrections[4] to (the self-component of) the differential cross sections of $H_2O$ and $D_2O$ observed in steady state[70] and pulsed neutron[71] experiments. As an example we show in Fig. 17 the time-of-flight data of Soper and Silver[71] on $H_2O$ as measured by the 40° detector bank of the General Purpose Diffractometer (GPD) instrument at Los Alamos National Laboratory, together with the model calculations corresponding to the same conditions (incident spectrum, ratio of flight paths, detector efficiency) as in the experiment. Here, the measured differential cross section at each value of the scattering vector $Q$ results from a rather complex folding, between

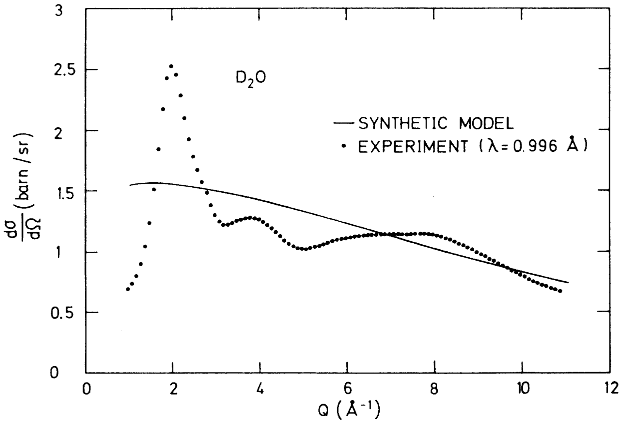

FIG. 18. Differential cross section of heavy water, as observed in a reactor experiment using neutrons of wavelength $\lambda=0.966$ Å (Ref. 70). The solid line is the result of the synthetic model calculation.

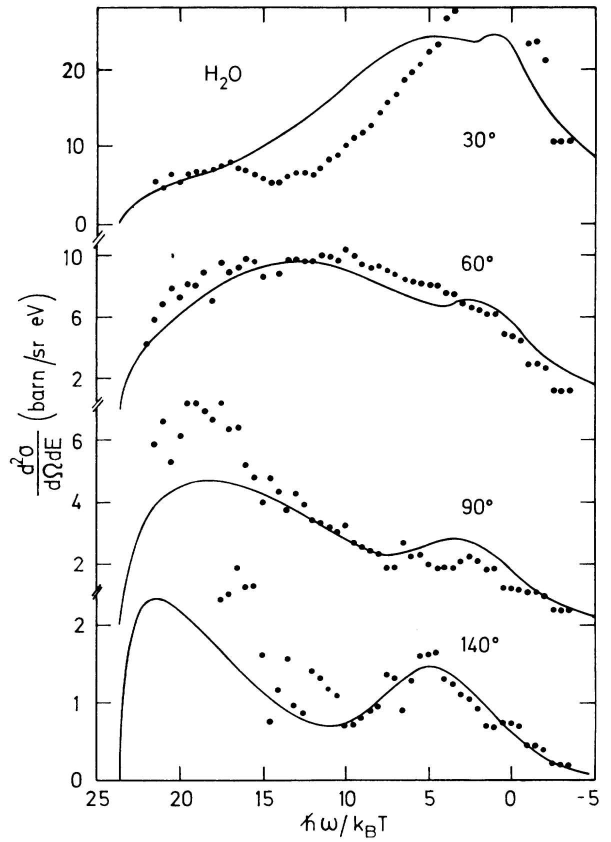

FIG. 19. The double-differential cross section of light water. The measured values are from Ref. 72. The solid lines correspond to the synthetic model results.

the above-mentioned experimental parameters and the actual scattering law of the scatterer. As a consequence, a strong variation of the measured curve with $Q$ arises in this case, which is still well reproduced by the model calculations.

The data of a reactor experiment on $D_2O$ performed by Soper and Phillips[70] are shown in Fig. 18, together with the evaluated curve from the synthetic scattering function. Due to its incoherent character, the latter can only give the pedestal over which the coherent contribution is superimposed.

Finally, we show in Fig. 19 the double-differential cross section of light water, as measured by Harling[72] and calculated according to the model under the same conditions as in that experiment. Although the synthetic function was not intended to describe the actual (self-) scattering law, but rather to produce good representations of some integral properties of it, there is a fair agreement between the measured and calculated curves.

## V. CONCLUSIONS

The analytical expressions derived from the synthetic model have been applied to the evaluation of several quantities of interest in neutron and reactor physics. The liquids $H_2O$, $D_2O$, and $C_6H_6$ were chosen as examples simply because a large amount of information there exist on them, thus providing a stringent test for the model. In each case, the result from the comparison with experimental data is highly encouraging, as it was possible to reproduce—in a fast and accurate way—measured values under a variety of conditions. Neutron scattering and thermalization properties of polyethilene have been also successfully described by the model.[73]

The ability of the synthetic function to generate inelastic, angular, and total cross sections, using a minimum set of input data (Table I) and with no adjustable parameters, could be very useful for the purpose of calculating neutron spectra and time-response functions in moderators. Besides these, other obvious applications of the model involve correction procedures, such as inelasticity effects in neutron diffraction work or multiple scattering calculations, in which a detailed knowledge of the first-order effects is not required. Work is in progress along these lines.

---

[1] J. R. Granada, Phys. Rev. B **31**, 4167 (1985).

[2] J. R. Granada, V. H. Gillettte, and R. E. Mayer, preceding paper, Phys. Rev. A **36**, 5585 (1987).

[3] J. U. Koppel and J. A. Young, Nukleonik **7**, 408 (1965).

[4] J. R. Granada, V. H. Gillette, and R. E. Mayer, Physica B **142**, 223 (1986).

[5] J. R. Granada, Phys. Rev. B **32**, 7555 (1985).

[6] G. I. Bell and S. Glasstone, *Nuclear Reactor Theory* (Van Nostrand Reinhold, New York, 1970), Chap. 4.

[7] J. U. Koppel, J. R. Triplett, and Y. D. Naliboff, General Atomic Report No. GA-7417 (Rev.), 1967 (unpublished).

[8] H. C. Honeck and Y. D. Naliboff, Argonne Computer Center, Reference Material Abstract No. 247, Argonne National Laboratory, Argonne, 1966 (unpublished).

[9] We are indebted to M. J. Abbate and M. M. Sbaffoni for supplying their results of GASKET and FLANGE runs.

[10] S. B. Herdade, M. J. Bechara, C. Rodriguez, and L. A. Vinhas, EXFOR Library Accession No. 30229 (Nuclear Data Section, IAEA, Vienna, 1973).

[11] J. M. Neill, J. L. Russell, Jr., and J. R. Brown, Nucl. Sci. Eng. **33**, 265 (1968).

[12] D. Garber, Brookhaven National Laboratory Report No. BNL-NCS-17541 (ENDF-201), 2nd ed., 1975 (unpublished).

[13] M. Nelkin, Phys. Rev. **119**, 741 (1960).

[14] J. U. Koppel and J. A. Young, Nucl. Sci. Eng. **19**, 412 (1964).

[15] R. M. Bansal, S. P. Tewari, and L. S. Kothari, J. Phys. D **7**, 1132 (1974).

[16] M. I. Markovic, Nucl. Instrum. Methods **195**, 597 (1982).

[17] F. Kropff, J. R. Latorre, J. R. Granada, and C. Castro Madero, EXFOR Library Accession No. 30283 (Nuclear Data Section, IAEA, Vienna, 1974).

[18] A. T. D. Butland and C. T. Chudley, J. Br. Nucl. Energy Soc. **13**, 99 (1974).

[19] D. Sprevak, G. M. Borgonovi, G. W. Carriveau, and J. M. Neill, General Atomic Report No. GA-8185, 1967 (unpublished).

[20] R. S. Marsden and H. L. McMurry, in *Proceedings of the Symposium On Neutron Thermalization and Reactor Spectra,*

*Ann Arbor, Michigan,* edited by M. Brown (STI/PUB/160, IAEA, Vienna, 1968), Vol. I, p. 457.

[21] H. L. McMurry, G. J. Russell, and R. M. Brugger, Nucl. Sci. Eng. **25**, 248 (1966).

[22] J. R. Beyster, Nucl. Sci. Eng. **31**, 254 (1968).

[23] S. Kornbichler, Nukleonik **7**, 281 (1965).

[24] J. R. Beyster *et al.*, General Atomic Report No. GA-6824, 1965 (unpublished).

[25] C. Hofmeyr, Nukleonik **7**, 286 (1965).

[26] V. C. Boffi, B. Marsico, V. G. Molinari, and R. Scozzafava, Nucl. Sci. Eng. **24**, 211 (1966).

[27] H. D. Lemmel, Nukleonik **7**, 265 (1965).

[28] M. C. Paiano and S. Paiano, in *Proceedings of the Symposium on Neutron Thermalization and Reactor Spectra, Ann Arbor, Michigan,* edited by M. Brown (STI/PUB/160, IAEA, Vienna, 1968), Vol. II, p. 395.

[29] E. Martinho and M. M. Costa Paiva, Nucl. Sci. Eng. **45**, 308 (1971).

[30] R. A. Bowen and M. C. Scott, J. Phys. D **2**, 401 (1969).

[31] D. Cokinos, E. Melkonian, and W. W. Havens, Jr., Trans. Am. Nucl. Soc. **12**, 669 (1969).

[32] P. B. Parks, D. J. Pellarin, N. H. Prochnow, and N. P. Baumann, Nucl. Sci. Eng. **33**, 209 (1968).

[33] J. Elkert, Nukleonik **11**, 159 (1968).

[34] E. Gon, L. Lidofsky, and H. Goldstein, Trans. Am. Nucl. Soc. **8**, 274 (1965).

[35] D. Freed and G. A. Whan, Trans. Am. Nucl. Soc. **8**, 433 (1965).

[36] L. Pal, E. Kisdi-Koszo, L. Bod, Z. Szatmary, and I. Vizi, in *Proceedings of the Third Geneva Conference on the Peaceful Uses of Atomic Energy* (United Nations, Geneva, 1964), Vol. 2, p. 310.

[37] R. M. Bansal, S. P. Tewari, and L. S. Kothari, Nucl. Sci. Eng. **69**, 367 (1979).

[38] J. Dorning, Nucl. Sci. Eng. **41**, 22 (1970).

[39] A. J. H. Goddard and P. W. Johnson, Nucl. Sci. Eng. **37**, 127 (1969).

[40] A. Ghatak and H. Honeck, Nucl. Sci. Eng. **21**, 227 (1965).

[41] W. W. Clendenin, Nucl. Sci. Eng. **18**, 351 (1964).

[42] J. R. Beyster *et al.*, General Atomic Report No. GA-2544, 1961 (unpublished).

[43] S. F. Nassar and G. Murphy, Nucl. Sci. Eng. **35**, 70 (1969).

[44] M. G. Silk and B. O. Wade, J. Nucl. Energy **23**, 1 (1969).

[45] R. B. Perez, M. J. Ohanian, and J. H. Dunlap, in *Proceedings of the Symposium on Neutron Thermalization and Reactor Spectra, Ann Arbor, Michigan,* edited by M. Brown (STI/PUB/160, IAEA, Vienna, 1968), Vol. II, p. 363.

[46] J. W. Daughtry and A. W. Waltner, in *Proceedings of the Symposium on Pulsed Neutron Research, Karlsruhe* (STI/PUB/104, IAEA, Vienna, 1965), Vol. I, p. 65.

[47] H. G. Jones, A. Robeson, and G. N. Salaita, Trans. Am. Nucl. Soc. **8**, 431 (1965).

[48] B. K. Malaviya and A. E. Profio, Trans. Am. Nucl. Soc. **6**, 58 (1963).

[49] G. Kussmaul and H. Meister, J. Nucl. Energy A/B **17**, 411 (1963).

[50] F. R. Westfall and A. W. Waltner, Trans. Am. Nucl. Soc. **5**, 386 (1962).

[51] N. P. Baumann, Nucl. Sci. Eng. **14**, 179 (1962).

[52] N. K. Ganguly and A. W. Waltner, Trans. Am. Nucl. Soc. **4**, 282 (1961).

[53] R. M. Bansal, S. P. Tewari, and L. S. Kothari, Nucl. Sci. Eng. **76**, 18 (1980).

[54] M. J. Abbate and J. Lolich, Atomkernenergie/K **33**, 195 (1979).

[55] H. C. Honeck and P. Michael, Nucl. Sci. Eng. **16**, 140 (1963).

[56] M. O. Caceres and H. S. Wio, Atomkernenergie/K **42**, 277 (1983).

[57] N. G. Sjöstrand, Ark. Fys. **15**, 145 (1959).

[58] K. H. Beckurts and K. Wirtz, *Neutron Physics* (Springer, Berlin, 1965).

[59] S. N. Purohit and N. G. Sjöstrand, in *Proceedings of the Symposium on Pulsed Neutron Research, Karlsruhe* (STI/PUB/104, IAEA, Vienna, 1965), Vol. I, p. 289.

[60] J. V. Lolich and M. J. Abbate, Atomkernenergie/K **35**, 23 (1980).

[61] L. Sancho and F. Verdaguer, An. R. Soc. Esp. Fis. Quim. Ser. A LXIII-A, 351 (1967).

[62] M. Küchle and G. Kussmaul, Nukleonik **6**, 329 (1964).

[63] F. Sefidvash, Atomkernenergie/K **42**, 191 (1983).

[64] H. S. Wio, Atomkernenergie/K **38**, 199 (1981).

[65] D. Sprevak, Ph.D. thesis, University of Cuyo, 1969 D. Sprevak, G. M. Borgonovi, J. M. Neill, and G. W. Carriveau, Nukleonik **11**, 233 (1968).

[66] J. R. Granada, V. H. Gillette, and R. E. Mayer, J. Nucl. Mater. **139**, 158 (1986). A small systematic discrepancy with the present results is due to the use now of a different (latest recommended) set of values for the bound cross sections.

[67] The density of heavy water as a function of temperature was taken from Table 15 in Ref. 18.

[68] P. A. Egelstaff, Adv. Chem. Phys. **53**, 1 (1983).

[69] G. Placzek, Phys. Rev. **86**, 377 (1952).

[70] A. K. Soper and M. G. Phillips, Chem. Phys. (to be published).

[71] A. K. Soper and R. N. Silver, Phys. Rev. Lett. **49**, 471 (1982).

[72] O. K. Harling, Pacific Northwest Laboratory, Report No. BNWL-436, 1967 (unpublished).

[73] J. Dawidowski, J. R. Granada, R. E. Mayer, and V. H. Gillette, Nucl. Instrum. Methods (to be published).